12-1-2020

Properties and performance of the basalt-fiber reinforced texture roof tiles

Parinya Chakartnarodom
Kasetsart University

Wichit Prakaypan
Shera Public Company Limited

Pitcharat Ineure
Glass Bridge Company Limited

Nutthita Chuankrerkkul
Chulalongkorn University

Edward A. Laitila
Michigan Technological University, ealaitil@mtu.edu

See next page for additional authors

Follow this and additional works at: https://digitalcommons.mtu.edu/michigantech-p
Part of the Materials Science and Engineering Commons

Authors
Parinya Chakartnarodom, Wichit Prakaypan, Pitcharat Ineure, Nutthita Chuankrerkkul, Edward A. Laitila, and Nuntaporn Kongkajun

Case Studies in Construction Materials 13 (2020) e00444

Contents lists available at ScienceDirect

Case Studies in Construction Materials

journal homepage: www.elsevier.com/locate/cscm

Case study

Properties and performance of the basalt-fiber reinforced texture roof tiles

Parinya Chakartnarodom[a], Wichit Prakaypan[b], Pitcharat Ineure[c], Nutthita Chuankrerkkul[d], Edward A. Laitila[e], Nuntaporn Kongkajun[f,*]

[a] Department of Materials Engineering, Faculty of Engineering, Kasetsart University, Chatuchak, Bangkok, 10900, Thailand
[b] Shera Public Company Limited, Pattananikom, Lopburi, 15220, Thailand
[c] Glass Bridge Company Limited, Ladphrao, Bangkok, 10230, Thailand
[d] Metallurgy and Materials Science Research Institute, Chulalongkorn University, Patumwan, Bangkok, 10330, Thailand
[e] Department of Materials Science and Engineering, Michigan Technological University, Houghton, MI, 49931, USA
[f] Department of Materials and Textile Technology, Faculty of Science and Technology, Thammasat University, Klong Luang, Pathumthani, 12121, Thailand

ARTICLE INFO

Article history:
Received 9 May 2020
Received in revised form 4 September 2020
Accepted 2 October 2020

Keywords:
Basalt
Composite materials
Roof tiles
Construction materials
Mechanical properties
Fiber-cement products

ABSTRACT

The mechanical and the physical properties, and the performance of texture roof tiles reinforced with the basalt fibers were observed. The samples of the basalt-fiber reinforced texture roof tiles were produced on the industrial scale by using filter pressing method. After forming, the as-molded samples were air cured and characterized based on ASTM C1185 standard for their mechanical properties and physical properties. In addition, the roof-tile installation test was also performed.

The results showed that the samples of the basalt-fiber reinforced texture roof tile (BFRT) could be produced on the industrial scale by using the common setting of the forming machine without further adjustment. For the appearance, the samples of BFRT had the appearance alike the common texture-roof tile products. In addition, BFRTs could be cut and drilled by using the standard cutting machine and could be installed by using the standard procedure for texture roof tile installation. For the properties, BFRTs had the properties as required by the industry requirements including the modulus of rupture (MOR) greater than 5 MPa, the modulus of elasticity (MOE) greater than 7000 MPa, the impact resistance greater than 1000 J/m^2, and the density between 1.5−2.2 g/cm^3.

1. Introduction

Texture roof tiles are generally used for roofing systems of traditional homes, hotel, or resort construction due to their attractive appearance and properties such as high strength and high durability, and their resistance to pest and insect. Normally, the strength of a roof tile is improved by reinforcing with the fibers. Previously, the common material used in the building material industry as the reinforcement phase was asbestos, a group of natural mineral fibers, owing to their properties such as high strength and heat stability [1–3]. It was found that the diameter and length of the asbestos could be reduced by a grinding process [4]. According to Hywang [5], asbestos could break down into the respirable airborne particles. For asbestos-containing building materials, the asbestos fibers can be released from the materials during dismantling [3,6,7].

* Corresponding author.
E-mail address: n-kongkj@tu.ac.th (N. Kongkajun).

https://doi.org/10.1016/j.cscm.2020.e00444

According to a report by International Agency for Research on Cancer (IARC) [1], the long term human exposure to asbestos would result in the diseases such as lung cancer, and mesothelioma. Currently, asbestos is banned by many countries such as Japan, Australia, United Kingdom, and many European countries. For fiber-reinforced building materials, the cellulose fibers and the synthetic polymeric fibers are the common asbestos-substitute materials [8]. However, the strength of those fibers is lower than asbestos [9–11]. In addition, both cellulose fibers and synthetic polymeric fibers are not heat resistant.

Basalt is a type of volcanic rock. Their chemical composition is primarily silicon oxide (SiO_2), aluminum oxide (Al_2O_3), calcium oxide (CaO), magnesium oxide (MgO), and other oxides depending on their geographic location [12–15]. In Thailand, basalt is highly abundant in the central region, eastern region, and northeast region. In those regions, the total basalt reserve is about 360 million tons; currently, there are more than 40 basalt mines in operation [16]. Presently, the basalt price from the mine is about $13/ton. Generally, basalt is used as an aggregate for road construction. However, Binici et al. [12] found that partial replacement of cement by basalt powder or basalt sand in concrete improved the concrete properties showing an increase of compressive strength and a decrease of water permeability.

Naturally, the hardness of basalt is between 5–9 on Mohr's scale [17]. Basalt could be melted and drawn into fiber using the fiber-extrusion process similar to glass fiber production [9,14,15,17]. General properties of basalt fibers are high strength, durability, high modulus of elasticity, high thermal stability ranging from $-200\,^{\circ}C$ to $700\,^{\circ}C$, sound insulation, high vibration resistance, nontoxic, and noncarcinogenic [9,14,17–20]. In addition, the basalt fibers have good alkaline resistant after being soaked in the 1 M calcium hydroxide ($Ca(OH)_2$) solution for 28 days [21].

Currently, there are many studies on the application of basalt fiber as a reinforcement phase in construction materials. For concrete, it was found that the mechanical properties such as the compressive strength, modulus of rupture (MOR), impact resistance, and freeze-thaw resistance of the concrete were improved by the addition of basalt fibers [9,20,22–24]. From Saloni et al. [25] and Punurai et al. [26], basalt fibers could improve the strength of geopolymer paste and also increased their setting time. Moreover, Li et al. [27] found that the performance of asphalt mixture under freezing conditions was improved by the incorporating of basalt fibers into the asphalt mixture.

Texture roof tiles are an example of fiber-cement products. Fiber-cement products are the fiber-reinforced building materials which also includes wall, ceiling, floor, and decorative applications. Fiber-cement products are often called “synthetic wood” or “artificial wood” by the consumers because they can be produced to have the wood-like texture and color and employed as a wood substitute for various applications in construction. Normally, the processes such as Hatschek process or filter pressing are utilized to produce the fiber-cement products from a slurry prepared from a mixture of ordinary Portland cement (OPC), fibers, sand, fillers, additives, and water.

Prior work [21] established the feasibility of using basalt fibers for fiber-cement products on the industrial scale. Basalt-fiber reinforced fiber-cement boards were produced on an industrial scale using the Hatschek process. Mechanical test showed that the fiber-cement boards had the strength as required by the Thai industrial standard (TIS) 1427-2540 and ASTM C1186 for flat non-asbestos fiber-cement sheets [28,29]. Current study mainly focuses on the applications of basalt fibers in another fiber-cement product. Basalt-fiber reinforced texture roof tiles (BFRT) were prepared on the industrial scale using filter pressing method and characterized for their mechanical and physical properties to understand if these meet or exceed Thai industrial standards. The effects of fiber content and length were observed. In addition, the installation test of the roof-tile samples and cost analysis were also carried out.

Fig. 1. Samples of BFRT.

2. Experimental

The samples of BFRT, Fig. 1, were produced on the industrial level at Shera Public Company Limited, Lop Buri, the leading non-asbestos fiber-cement manufacturer in Thailand.

Tables 1 and 2 show the formulas used to prepare the dry mixtures, mixed by weight. The dry mixtures prepared from formula A1 to A5 on Table 1 and formula R1 to B5 on Table 2 were mixed with water to form a slurry. The water content in the slurry was about 30 wt%. Roof-tile samples were then produced on the industrial scale from the slurry by the filter pressing method. The basalt fibers used in this work were produced from a mixture of basalt rock, limestone, and cullet. The diameter of the basalt fibers was about 15 μm. Prior to mixing with other raw materials, basalt fibers were ground by ball milling for 8 h to produce short basalt fibers, and then sieved using the sieve shaker. The sieve sizes were 30, 80, 100, 230, and 325 mesh which correspond to the sieve opening of 600, 180, 150, 63, and 45 μm, respectively. The ground basalt fibers that passed 30-mesh sieve but remained on 80-mesh sieve were used in Formula A1 in Table 1. Based on the sieve opening size, length range of the basalt fibers used to produce the roof tile samples from fomula A1 to A5 in Table 1 were 180–600 μm, 150–180 μm, 63–150 μm, 45–63 μm, and < 45 μm, respectively.

According to our previous work [21], using short basalt fibers improved the compatibility of basalt fibers to the fiber-cement production process used by the factory, increased the formability of the basalt reinforced fiber-cement products, and the interfacial bonding between basalt fibers and cement matrix. Because the basalt fibers are naturally brittle, producing the short basalt fibers in the factory can be simply done by grinding process.

Pigment was used as the additive to provide color to the roof- tile samples. Limestone, gypsum, and fly ash were generally used as the fillers to improve the properties such as packing efficiency, and toughness of the roof tiles, and the flowability of the mixture during the roof-tile forming process. For cellulose and polyester fibers, they were used to assist the roof-tile forming process and provide additional flexibility to the roof tiles. The size of the limestone used in both Tables 1 and 2 was smaller than 200 mesh or 74 μm. The effect of basalt fiber content change was also determined, Table 2, where Formula R1 is a common formula for producing the texture roof tiles. Therefore, the roof tiles samples produced from Formula R1 were used as the reference samples. In Formula B1 to B5, the amount of basalt fibers with the same length range were changed. In Formula B1 and B2, compared with Formula R1, polyvinyl alcohol (PVA) fibers were partially and fully replaced with basalt fibers. In Formula B3 to B5, basalt fibers were further added to replace cellulose fibers.

After molding, the roof-tile samples were air cured for 7 days, the maximum inventory period for the air-cured fiber-cement products used at the factory. The roof-tile samples were characterized for bulk density, modulus of rupture (MOR), modulus of elasticity (MOE), and impact resistance. Ten samples were used for each test. The characterization process was based on ASTM C1185 standard [30]. Archimedes method was used to measure the bulk density. Three-point bend test was used to measure MOR and MOE. Pendulum impact tester was used to measure impact resistance. X-ray fluorescence (XRF) spectrometer and X-ray powder diffractometer (XRD) were used to determine the chemical composition and the structure of basalt fibers. Scanning electron microscopy (SEM) was used to observe the microstructure of the roof-tile samples. Installation test of the BFRT was also carried out.

Statistical hypothesis tests using t- distribution were used to compare the mean values of each property with the industrial requirement of that property. The equations used for the analysis are shown in Table 3, where; μ is the mean, n is the sample size, $\bar{x}$ is the sample mean, s and s^2 are the sample standard deviation and the sample variance, and a_1 is a constant. The level of significance (α) used for the statistical hypothesis test is 0.05. Null hypothesis is rejected if P-value is less than α. Theoretically, the P-value is the minimum α required to reject the null hypothesis which is calculated from the probability at which the value of test statistic T is greater than $(\bar{x} - a_1)/(s/\sqrt{n})$ from t-distribution. The full details of the statistical hypothesis test can be seen from Walpole et al. [31], Montgomery and Runger [32], and Devore [33].

The equations used for statistical hypothesis test concerning mean difference between two sets of samples are shown in Table 4. The subscript 1 and 2 are for sample set 1 and 2 respectively. The P-value in this case is still calculated from the value of T which is the probability at which $|T| > (\bar{x}_1 - \bar{x}_2)/\sqrt{(s_1^2/n_1 + s_2^2/n_2)}$.

Table 1
Formula for producing BFRTs. The effects of the basalt fiber length on the properties of roof-tile samples were observed.

Materials	Formula (wt%)				
	A1	A2	A3	A4	A5
Basalt fibers	0.4	0.4(80–100)(150–180)	0.4(100–230)(63–150)	0.4(230–325)(45–63)	0.4
(fiber length range, mesh no.)	(30–80)				(< 325)
(fiber length range, μm)	(180–600)				(< 45)
Ordinary Portland cement (OPC)	48.7	48.7	48.7	48.7	48.7
Limestone	17.0	17.0	17.0	17.0	17.0
Gypsum	5.0	5.0	5.0	5.0	5.0
Fly ash	26.7	26.7	26.7	26.7	26.7
Pigment	1.1	1.1	1.1	1.1	1.1
Cellulose fibers	1.0	1.0	1.0	1.0	1.0
Polyester fibers	0.1	0.1	0.1	0.1	0.1

Table 2
Formula for producing BFRTs. The effects of basalt fiber content on the properties of roof-tile samples were observed.

Materials	Formula (wt%)					
	R1	B1	B2	B3	B4	B5
Basalt fibers	0	0.25	0.5	0.75	1	1.25
OPC	49	49	49	49	49	49
Limestone	48.5	48.5	48.5	48.5	48.5	48.5
Pigment	1	1	1	1	1	1
Cellulose fibers	1	1	1	0.75	0.5	0.25
PVA fibers	0.5	0.25	0	0	0	0

Table 3
Statistical hypothesis test concerning mean [31].

Null hypothesis (H_0)	Alternative hypothesis (H_1)	Degree of freedom (ν)	Value of test statistic (T)
$\mu = a_1$	$\mu > a_1$	$\nu = n - 1$	$T = \frac{\bar{x}-a_1}{s/\sqrt{n}}$

Table 4
Statistical hypothesis test concerning mean difference between two sets of sample [31].

Null hypothesis (H_0)	Alternative hypothesis (H_1)	Degree of freedom (ν)	Value of test statistic (T)
$\mu_1 = \mu_2$	$\mu_1 \neq \mu_2$	$\nu = \frac{\left(s_1^2/n_1+s_2^2/n_2\right)^2}{\frac{\left(s_1^2/n_1\right)^2}{(n_1-1)}+\frac{\left(s_2^2/n_2\right)^2}{(n_2-1)}}$	$T=\frac{\bar{x}_1-\bar{x}_2}{\sqrt{\left(s_1^2/n_1+s_2^2/n_2\right)}}$

3. Results and discussion

3.1. Basalt fibers

From the XRD pattern, Fig. 2, there is only broad peak indicating the basalt fibers are amorphous. The chemical composition based on XRF analysis determined the basalt fibers primarily consisted of silicon oxide (SiO_2) calcium oxide (CaO), and aluminum oxide (Al_2O_3), Table 5. When the fibers were ground and used to produce the roof-tile samples, the ground basalt fibers had a straight cylindrical shape with a uniform diameter and fractured only on the transverse direction, Fig. 3. This indicated the brittle fracture behavior [34] of the basalt fibers which agreed with the experiment by Militky and Kovacic [13]. Typically, the man-made vitreous fibers having the amorphous structure will not break lengthwise because there is no cleavage plane in the structure [4,35]. Therefore, when the basalt fibers are fractured by the grinding process, the fibers only become shorter while retaining their original diameter [36].

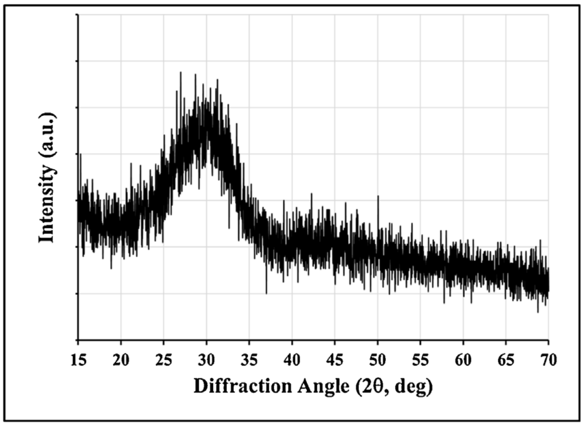

Fig. 2. X-ray diffraction pattern of the basalt fibers.

Table 5
Chemical composition of basalt fibers.

Chemical Composition (wt%)						
SiO_2	**CaO**	**Al_2O_3**	**MgO**	**TiO_2**	**Fe_2O_3**	**SO_3**
36.9	39.72	14.9	4.9	0.751	0.705	0.63
BaO	**K_2O**	**MnO**	**SrO**	**ZrO_2**	**CuO**	**Others**
0.53	0.44	0.27	0.118	0.051	0.032	0.053

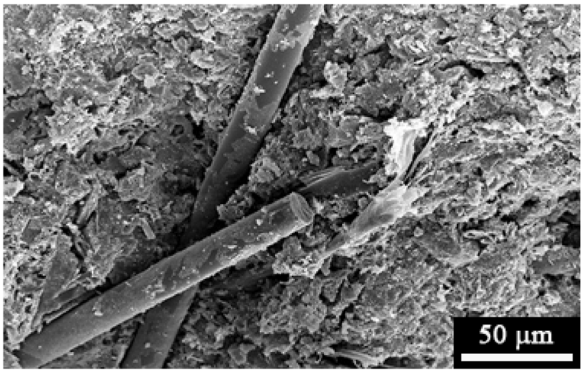

Fig. 3. Ground basalt fibers in the cement matrix of BFRT.

3.2. General characteristics of the BFRTs

The samples of BFRT could be produced on the industrial scale using the roof-tile forming machine without further adjustment of the production parameters. Beside the strength, the attractive appearance is a very important feature for texture roof tiles and other fiber-cement products. Obviously, from Fig. 4, BFRT with a fine texture surface can be produced. In addition, as shown on Fig. 5(a), the roof-tile samples could be cut using an angle grinder, a common fiber-cement cutting tool for the construction workers. The cutting edge by angle grinder was smooth without any cracks or failures. Furthermore, without difficulty, the roof-tile samples could be drilled and affixed on the rail by using screws as shown on Fig. 5(b). For the installation test, Fig. 6, the roof-tile samples could be installed using the standard method for texture roof tile installation. No installation problems were observed.

3.3. Properties of BFRTs

The properties of roof-tile samples including bulk density, MOR, MOE, and impact resistance are provided in Fig. 7. The dash line represented the values based on the industry requirements listed in Table 6 [37]. Noticeably, bulk density of the roof-tile samples from all length ranges satisfied the industrial requirement which is between 1.5–2.2 g/cm^3. However, the average MOR of the roof-tile samples produced using the basalt fibers from the length range 150–180 μm (Formula A2), and 180–600 μm (Formula A1) were less than 5 MPa which did not satisfy the requirement. Hence, the statistical hypothesis

Fig. 4. The surface appearance of BFRT.

(a)

(b)

Fig. 5. BFRT (a) cutting and (b) drilling.

Fig. 6. Installation test of BFRTs.

tests in Tables 7–9 focus only on the basalt fibers having length range < 45 μm (Formula A5), 45–63 μm (Formula A4), and 63–150 μm (Formula A3)

By observing the P-values from Tables 7–9, only the P-values from length range 45–63 μm and 63–150 μm are less than 0.05 in all tables. Therefore, according to the P-values, only the roof-tile samples produced from formula A3 (length range 63–150 μm) and A4 (length range 45–63 μm) satisfied the industrial requirement on MOR, MOE, and impact resistance.

The statistical hypothesis test regarding mean comparisons on MOR, MOE, and impact resistance between the length range 45–63 μm and 63–150 μm are shown in Table 10. Because the P-values are greater than 0.05 for all mechanical

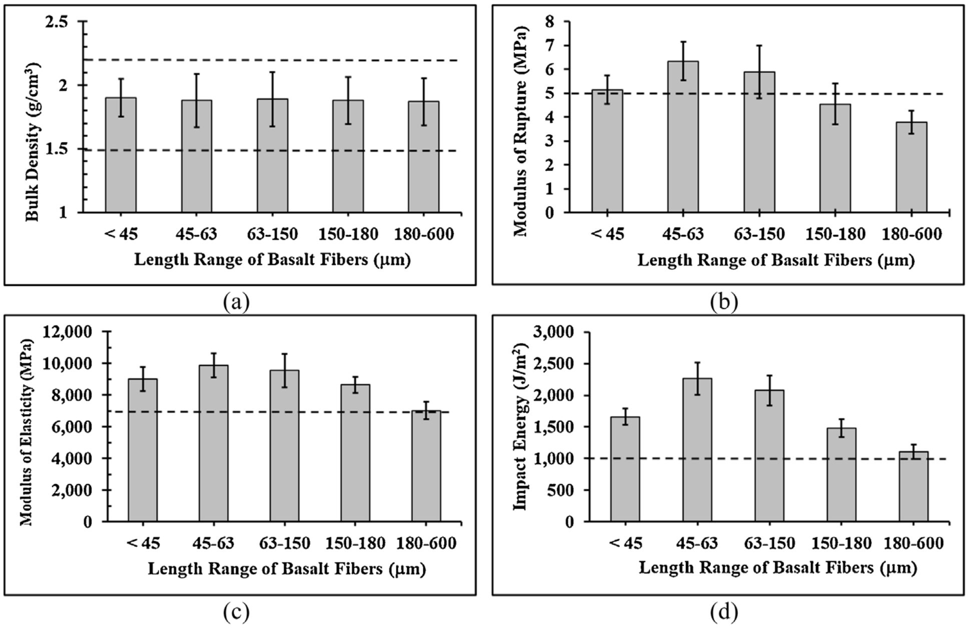

Fig. 7. The properties of BFRT from Formula A1 to A5 (a) bulk density (b) MOR (c) MOE (d) impact resistance. The horizontal dash line on each graph indicates the requirement for each properties based on the values shown on Table 6.

Table 6
Required properties of the texture roof tile [37].

Properties	Requirement
Modulus of rupture (MOR)	greater than 5 MPa
Modulus of elasticity (MOE)	greater than 7000 MPa
Impact resistance	greater than 1000 J/m^2
Bulk density	between 1.5–2.2 g/cm^3

Table 7
Statistical analysis on MOR for the samples of BFRT.

H0:	μ_{MOR} = 5 MPa					
H1:	μ_{MOR} > 5 MPa					
Length range (μm)	Mean (MPa)	Variance (MPa^2)	Sample size	Degree of freedom	T	P-Value
< 45 (Formula A5)	5.15	0.365	10	9	0.785	0.2263
45–63 (Formula A4)	6.34	0.647	10	9	5.27	2.58×10^{-4}
63–150 (Formula A3)	5.89	1.209	10	9	2.56	0.0154
Decision:	The average MOR of length range 45–63 μm and 63–150 μm are significantly higher than 5 MPa because P-values of those length ranges are lower than 0.05.					

properties, there are no significant difference on mechanical properties between the roof-tile samples produced by using basalt fibers from both length range, 45–63 μm and 63–150 μm.

Generally, the interaction between the reinforcement phase and the matrix phase, such as physical adhesion, friction, and mechanical interlocking, change the effectiveness of the fibers in enhancing the mechanical properties of the composite materials [11,38,39]. Khandelwal and Rhee [40] mentioned that adhesion between the basalt fibers and the cement matrix was the important factor affecting the mechanical properties of the basalt-fibers reinforced composites. According to Guo et al. [24], the random 3D orientation of the basalt fibers could improve the fracture properties of the composites by hindering the cracks in the cement matrix. During the impact, the lowering of stress concentration at the crack tips due to the crack bridging by basalt fibers could facilitate the release of impact energy leading to the improved impact resistance [24]. According to Sun et al. [41], shorter basalt fibers was more effective in improving the strength of the composites.

Table 8
Statistical analysis on MOE for the samples of BFRT.

H0:	μ_{MOE} = 7000 MPa					
H1:	μ_{MOE} > 7000 MPa					
Length range (μm)	Mean (MPa)	Variance (MPa^2)	Sample size	Degree of freedom	T	P-Value
< 45 (Formula A5)	9011	5.91×10^5	10	9	8.27	8.46×10^{-6}
45–63 (Formula A4)	9866	6.06×10^5	10	9	11.64	4.97×10^{-7}
63–150 (Formula A3)	9543	1.12×10^6	10	9	7.60	1.66×10^{-5}
Decision:	The mean MOE of all length ranges are significantly higher than 7000 MPa because P-values of those length ranges are lower than 0.05.					

Table 9
Statistical analysis on impact resistance for the BFRT.

H0:	μ_{Impact} = 1000 J/m^2					
H1:	μ_{Impact} > 1000 J/m^2					
Length range (μm)	Mean (J/m^2)	Variance (J^2/m^4)	Sample size	Degree of freedom	T	P-Value
< 45 (Formula A5)	1659	1.66×10^4	10	9	16.18	2.92×10^{-8}
45–63 (Formula A4)	2261	6.35×10^4	10	9	15.83	3.54×10^{-8}
63–150 (Formula A3)	2076	5.49×10^4	10	9	14.52	7.48×10^{-8}
Decision:	The mean impact resistance of all length ranges are significantly higher than 1000 J/m^2 because P-values of those length ranges are lower than 0.05.					

Table 10
Statistical analysis on mean difference between the properties of roof-tile samples produced from formula A3 (length range 63-150 μm) and A4 (length range 45-63 μm).

Property:	MOR	MOE	Impact resistance
H0:	$\mu_{A3} = \mu_{A4}$		
H1:	$\mu_{A3} \neq \mu_{A4}$		
Degree of freedom:	16.49	16.54	17.91
T:	1.04	0.78	1.70
P-Value:	0.31	0.45	0.11
Decision:	Because P-values are higher than 0.05 in all properties, the mean MOR, MOE, and impact resistance of the samples produced from both length range are not significantly difference.		

Therefore, in our case, when the basalt-fiber lengths were 45–150 μm, there was improvement of fiber and matrix adhesion which resulted in the improvement of MOR, MOE, and the impact resistance.

Results from MOR, MOE, and impact resistance of the samples of BFRT are provided in Fig. 8. The length range of the basalt fibers used to produce the samples in this case was 45–63 μm. The basalt fiber contents of 0.25 wt% (formula B1) and 0.50 wt % (formula B2), MOR, MOE, and the impact resistance of the roof tiles are comparable to the samples from control formula R1 (0 wt% basalt fibers).

At the basalt fiber content of 0.25 wt% and 0.50 wt%, the basalt fibers added substitute for the PVA fibers in formula R1. The statistical hypothesis test on mean comparison were conducted for MOR, MOE, and impact resistance between the roof-tile samples produced from formula R1 and formula B1 (0.25 wt% basalt fiber) or B2 (0.50 wt% basalt fiber) as shown in Table 11–13.

Based on statistical analysis, between the samples produced from formula R1 and formula B1 (fiber content 0.25 wt%), the MOR, MOE, and impact resistance of the roof-tile samples from formula B1 were not significantly different from formula R1 because P-values from all cases are greater than 0.05.

For fiber content of 0.50 wt%, P-values for MOR and impact resistance are greater than 0.05 while P-value for MOE is less than 0.05. Therefore, MOE of the roof tile samples from formula B2 was higher than MOE of the roof tile samples from formula R1. However, there were no significant difference on MOR and impact resistance between the samples from formula R1 and formula B2. According to the statistical analysis, basalt fibers could be used to replace PVA fibers in texture roof tiles without causing the negative impact on their MOR, MOE, and impact resistance.

When the basalt fiber content was greater than 0.5 wt% (formula B3 to B5), both MOR and impact resistance decreased but MOE increased, Fig. 8. Normally, based on the rule of mixture, when the amount of the fiber increases, MOE of the composite materials would increase. However, MOR and impact resistance were affected by the fiber-matrix interactions

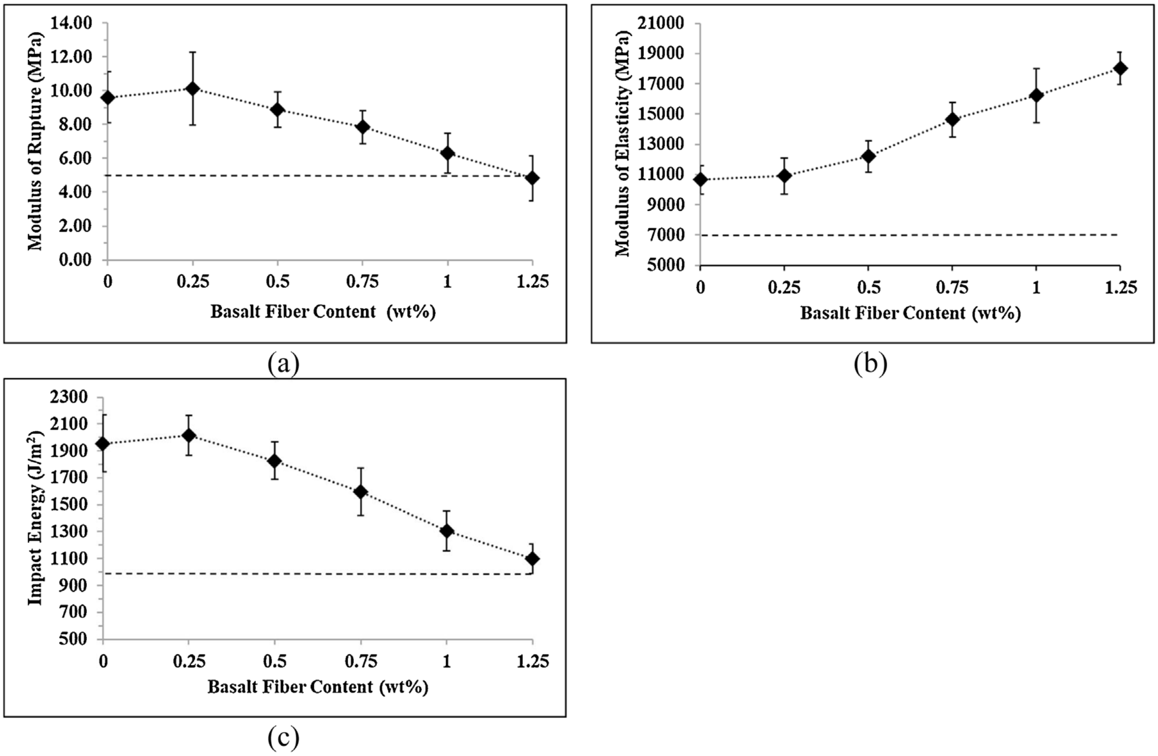

Fig. 8. The mechanical properties of BFRT from Formula R1 to B5 (a) MOR (b) MOE (c) impact resistance. The horizontal dash line on each graph indicates the requirement for each properties based on the values shown on Table 6. The length range of the basalt fibers in the samples was 45 - 63 µm.

Table 11
Statistical hypothesis for mean comparison on MOR.

Basalt fiber content (wt%)	Mean (MPa)	Variance (MPa^2)	Sample size
0 (Formula R1)	9.61	2.270	10
0.25 wt% (Formula B1)	10.12	4.591	10
0.50 wt% (Formula B2)	8.88	1.086	10
H_o	$\mu_1 = \mu_2$		
H_1	$\mu_1 \neq \mu_2$		
Comparison	Formula R1 vs. Formula B1		Formula R1 vs. Formula B2
Degree of freedom	16.15		16.01
Value of test statistic	−0.618		1.250
P-Value	0.545		0.230
Decision	Because P-values are higher than 0.05, average MOR of the samples from both fiber contents are not significantly difference.		Because P-values are higher than 0.05, average MOR of the samples from both fiber contents are not significantly difference.

[24,34,38,39,42]. According to Guo et al. [24], the performance reduction of the basalt -fiber reinforced cement composites could be from the clustering of basalt fibers in the composites and weak bonding between the basalt fibers and the cement matrix. From Fig. 3, the surface of basalt fibers was relatively smooth. Therfore, the overall bonding between cement matrix and basalt fibers was weaken when the amount of basalt fibers increased which resulted in the reduction of both MOR and impact resistance. In addition, when the basalt fiber content in BFRTs increased, the agglomeration of basalt fibers in BFRTs may be possible resulting in the reduction of MOR and impact resistance.

3.4. Cost analysis

As mentioned before, the price of basalt from the mine is about $13/ton. However, to produce basalt fibers, the operating costs such as labor cost, energy cost, and overhead cost must be considered. The estimated operating costs for producing basalt fibers based on the information from glass industry in Thailand are listed in Table 14. To produce 30 tons of basalt fibers in Thailand daily, it will cost at least $314/ton in the production.

Table 12
Statistical hypothesis for mean comparison on MOE.

Basalt fiber content (wt%)	Mean (MPa)	Variance (MPa^2)	Sample size
0 (Formula R1)	10,653.90	907,506	10
0.25 wt% (Formula B1)	10,905.40	1,407,907	10
0.50 wt% (Formula B2)	12,193.20	1,081,952	10
H_o	$\mu_1 = \mu_2$		
H_1	$\mu_1 \neq \mu_2$		
Comparison	Formula R1 vs. Formula B1	Formula R1 vs. Formula B2	
Degree of freedom	17.20	17.86	
Value of test statistic	−0.523	−3.45	
P-Value	0.608	0.0031	
Decision	Because P-values are higher than 0.05, average MOE of the samples from both fiber contents are not significantly difference.	Because P-values are lower than 0.05, average MOE of the samples from both fiber contents are significantly difference.	

Table 13
Statistical hypothesis for mean comparison on impact resistance.

Basalt fiber content (wt%)	Mean (J/m^2)	Variance (J^2/m^4)	Sample size
0 (Formula R1)	1954.70	44,772.90	10
0.25 wt% (Formula B1)	2015.00	21,202.22	10
0.50 wt% (Formula B2)	1827.50	20,130.28	10
H_o	$\mu_1 = \mu_2$		
H_1	$\mu_1 \neq \mu_2$		
Comparison	Formula R1 vs. Formula B1	Formula R1 vs. Formula B2	
Degree of freedom	15.96	15.73	
Value of test statistic	−0.742	1.579	
P-Value	0.470	0.135	
Decision	Because P-values are higher than 0.05, average impact resistance of the samples from both fiber contents are not significantly difference.	Because P-values are higher than 0.05, average impact resistance of the samples from both fiber contents are not significantly difference.	

Table 14
The estimated operating costs for producing basalt fibers at the capacity of 30 tons/day.

Cost Item	Cost ($/ton)
Energy	113
Labor	150
Overhead	38

According to the information from fiber-cement industry, the cost of each raw material is shown in Table 15. The total cost of each raw material used to produce 1 ton of texture roof tiles from formula R1 is provided in Fig. 9. Even though the total fiber content in formula R1 is only 1.5 wt%, the percentage of materials cost for the fibers is 40 %. Moreover, 31 % of the materials cost is from PVA fibers. Therefore, reducing the fiber cost is the key to reduce the total materials cost.

Assuming the price of basalt fibers is $623/ton which is twice of the production cost for basalt fibers, Fig. 10 shows the estimated cost per ton of raw materials to produce the texture roof tiles from formula R1 and B1-B5 in Table 2. The percentage of materials cost saving by using basalt fibers are graphed in Fig. 10. In the previous section, the statistical hypothesis test showed that basalt fibers could be used to replace PVA fibers. From Fig. 10, the cost saving is about 27 % at 0.5 wt% basalt fiber content. At 0.5 wt% basalt fiber content, PVA fibers in Formula R1 were fully replaced by basalt fibers, Table 2. Because PVA fibers have the highest unit cost, replacing PVA fibers with basalt fibers significantly impacts the materials cost, Fig. 10. Annually, the demand on PVA fibers in a fiber-cement factory is about 6000 tons to use in all fiber cement products and the price/ton of PVA is about $5313/ton. If the price/ton of the basalt fibers is $623/ton and the basalt fibers are used to substitute PVA fibers, the factory could save about 28 million dollars a year.

Summary

The aim of this work was to study the mechanical and the physical properties, and the performance of the basalt-fiber reinforced roof tiles (BFRTs). The results showed that:

Table 15
The estimated cost of the raw materials for producing the texture roof tiles from the formula listed on Table 2.

Raw Material	Cost ($/ton)
Ordinary Portland cement (OPC)	54
Limestone	22
Pigment	1563
Cellulose fibers	782
PVA fibers	5313

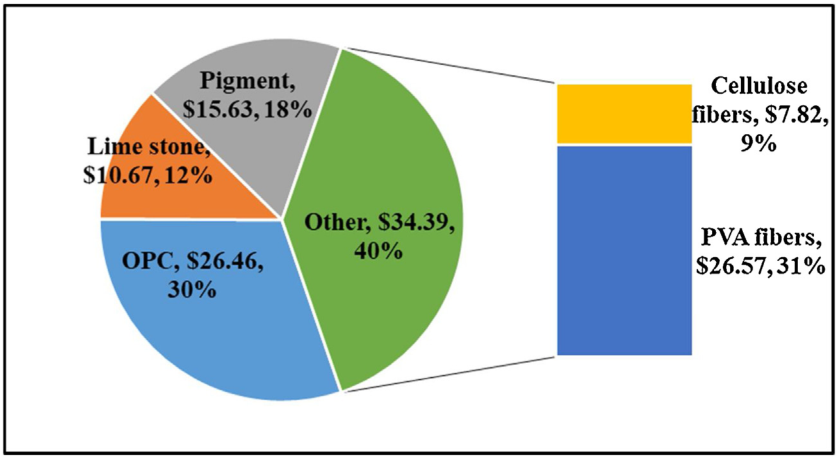

Fig. 9. The cost of raw materials used to produce one ton of texture roof tiles from formula R1.

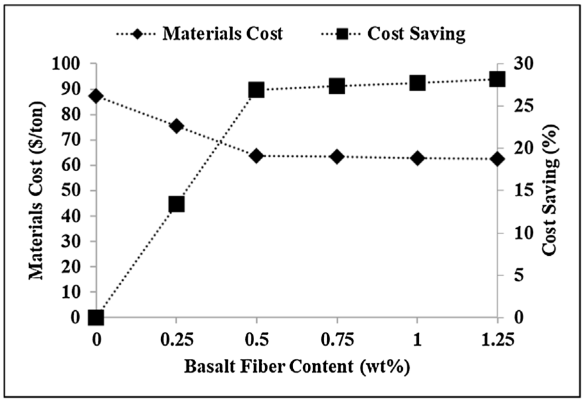

Fig. 10. The total cost per ton of the raw materials ($/ton) and % cost saving by using basalt fibers.

- BFRTs could be produced on the industrial scale by using the similar machine and setting for producing the regular texture roof tiles without further adjustment.
- BFRTs could be cut, drilled, and installed using the standard tools and the standard procedure for texture roof tile installation.
- BFRTs with fine texture surface could be produced.
- BFRTs produced from the basalt fibers with length range 45–150 μm had the properties as required by the industry requirements including the modulus of rupture (MOR) greater than 5 MPa, the modulus of elasticity (MOE) greater than 7000 MPa, the impact resistance greater than 1000 J/m^2, and the density between 1.5–2.2 g/cm^3.
- The size and amount of basalt fibers affected the mechanical properties of BFRTs.
- Using basalt fibers could be used to substitute PVA fibers leading to the reduction of the total materials cost for producing BFRTs.

Declaration of Competing Interest

The authors report no declarations of interest.

Acknowledgements

This work was supported by National Research Council of Thailand (NRCT), Shera Public Company Limited, and Glass Bridge Company Limited.

References

[1] IARC (International Agency for Research on Cancer), Arsenic, metals, fibres, and dusts: a review of human carcinogens, IARC Monogr. Eval. Carcinog. Risks Hum. 100C (2012).
[2] A. Franzblau, A.H. Demond, S.K. Sayler, H. D'Arcy, R.L. Neitzel, Asbestos-containing materials in abandoned residential dwellings in Detroit, Sci. Total Environ. 714 (2020)136580.
[3] A. Obmiński, Asbestos in building and its destruction, Constr. Build. Mater. 249 (2020)118685.
[4] J. Assuncao, M. Corn, The effects of milling on diameters and lengths of fibrous glass and chrysotile asbestos fibers, Am. Ind. Hyg. Assoc. J. 36 (11) (1975) 811–819.
[5] C.Y. Hywang, Size and shape of airborne asbestos fibres in mines and mills, Br. J. Ind. Med. 40 (3) (1983) 273–279.
[6] A. Obmiński, J. Janeczek, The effectiveness of asbestos stabilizers during abrasion of asbestos-cement sheets, Constr. Build. Mater. 249 (2020)118767.
[7] Y.C. Kim, Y.L. Zhang, W.J. Park, G.W. Cha, W.H. Hong, Quantifying asbestos fibers in post-disaster situations: preventive strategies for damage control, Int. J. Disaster Risk Reduct. 48 (2020)101563.
[8] S.H. Park, Types and health hazards of fibrous materials used as asbestos substitutes, Saf. Health Work 9 (3) (2018) 360–364.
[9] S.E. Mohammadyan-Yasouj, A. Ghaderi, Experimental investigation of waste glass powder, basalt fibre, and carbon nanotube on the mechanical properties of concrete, Constr. Build. Mater. 252 (2020)119115.
[10] H. Savastano, S.F. Santos, J. Fiorelli, V. Agopyan, 19 - sustainable use of vegetable fibres and particles in civil construction, in: J.M. Khatib (Ed.), Sustainability of Construction Materials, second edition, Woodhead Publishing, 2016, pp. 477–520.
[11] A. Bentur, S. Mindess, Fibre Reinforced Cementitious Composites, Taylor & Francis, New York, 2007.
[12] H. Binici, Y. Yardim, O. Aksogan, R. Resatoglu, A. Dincer, A. Karrpuz, Durability properties of concretes made with sand and cement size basalt, Sustain. Mater. Technol. 23 (2020)e00145.
[13] J. Militky, V. Kovacic, Ultimate mechanical properties of basalt filaments, Text. Res. J. 66 (4) (1996) 225–229.
[14] E. Monaldo, F. Nerilli, G. Vairo, Basalt-based fiber-reinforced materials and structural applications in civil engineering, Compos. Struct. 214 (2019) 246–263.
[15] G.L. Sheldon, Forming fibres from Basalt Rock, Platin. Met. Rev. 21 (1) (1977) 18–24.
[16] Thai Department of Primary Industries and Mines, Stone Sources for Industrial Utilization, (2020) . http://www1.dpim.go.th/qry/quarry3.php.
[17] H. Jamshaid, R. Mishra, A green material from rock: basalt fiber – a review, J. Text. Inst. 107 (7) (2016) 923–937.
[18] H. Katkhuda, N. Shatarat, Improving the mechanical properties of recycled concrete aggregate using chopped basalt fibers and acid treatment, Constr. Build. Mater. 140 (2017) 328–335.
[19] B.V. Perevozchikova, A. Pisciotta, B.M. Osovetsky, E.A. Menshikov, K.P. Kazymov, Quality evaluation of the Kuluevskaya Basalt outcrop for the production of mineral fiber, southern Urals, Russia, Energy Procedia 59 (2014) 309–314.
[20] C. Jiang, K. Fan, F. Wu, D. Chen, Experimental study on the mechanical properties and microstructure of chopped basalt fibre reinforced concrete, Mater. Des. 58 (2014) 187–193.
[21] P. Chakartnarodom, W. Prakaypan, P. Ineure, N. Kongkajun, N. Chuankrerkkul, Feasibility study of using basalt fibers as the reinforcement phase in fiber-cement products, Key Eng. Mater. (2018) 252–257.
[22] Z. Algin, M. Ozen, The properties of chopped basalt fibre reinforced self-compacting concrete, Constr. Build. Mater. 186 (2018) 678–685.
[23] A.B. Kizilkanat, N. Kabay, V. Akyüncü, S. Chowdhury, A.H. Akça, Mechanical properties and fracture behavior of basalt and glass fiber reinforced concrete: an experimental study, Constr. Build. Mater. 100 (2015) 218–224.
[24] Z.S. Guo, N. Hao, L.M. Wang, J.X. Chen, Review of basalt-fiber-Reinforced cement-based composites in China: their dynamic mechanical properties and durability, Mech. Compos. Mater. 55 (1) (2019) 107–120.
[25] Parveen Saloni, T.M. Pham, Enhanced properties of high-silica rice husk ash-based geopolymer paste by incorporating basalt fibers, Constr. Build. Mater. 245 (2020)118422.
[26] W. Punurai, W. Kroehong, A. Saptamongkol, P. Chindaprasirt, Mechanical properties, microstructure and drying shrinkage of hybrid fly ash-basalt fiber geopolymer paste, Constr. Build. Mater. 186 (2018) 62–70.
[27] Z. Li, A. Shen, H. Wang, Y. Guo, H. Wu, Effect of basalt fiber on the low-temperature performance of an asphalt mixture in a heavily frozen area, Constr. Build. Mater. 253 (2020)119080.
[28] TIS 1427-2540, Fibre-Cement Sheets: Flat Sheets, Thai Industrial Standards Institute (TISI), (1997) .
[29] ASTM C1186, Standard Specification For Flat Non-Asbestos Fiber-Cement Sheets ASTM International, West Conshohocken, PA.
[30] ASTM C1185, Standard Test Methods for Sampling and Testing Non-Asbestos Fiber-Cement Flat Sheet, Roofing and Siding Shingles, and Clapboards, ASTM International, West Conshohocken, PA.
[31] R.E. Walpole, R.H. Myers, S.L. Myers, K. Ye, Probability & Statistics for Engineers & Scientists, 9th ed., Prentice Hall, 2012.
[32] D.C. Montgomery, G.C. Runger, Applied Statistics and Probability for Engineers, 3rd ed., John Wiley & Sons, Inc., 2003.
[33] J.L. Devore, Probability and Statistics for Engineering and the Sciences, 8th ed., Cengage Learning, 2012.
[34] W.D. Callister Jr., D.G. Rethwisch, Materials Science and Engineering: An Introduction, Wiley, 2014.
[35] IARC (International Agency for Research on Cancer), Man-made vitreous fibres, IARC Monogr. Eval. Carcinog. Risks Hum. 81 (2002).
[36] J. Militký, V. Kovačič, J. Rubnerová, Influence of thermal treatment on tensile failure of basalt fibers, Eng. Fract. Mech. 69 (9) (2002) 1025–1033.
[37] TIS 535-2556, Concrete Roofing Tiles, Thai Industrial Standards Institute (TISI), Thailand, 2013.
[38] M.A. Meyers, K.K. Chawla, Mechanical Behavior of Materials, Cambridge University Press, New York, 2009.
[39] C. Mihael, D. Ramona, D.C. Laurentiu, The Impact Behaviour of Composite Materials 3rd International Conference on Maritime and Naval Science and Engineering, Romania, 2010.
[40] S. Khandelwal, K.Y. Rhee, Recent advances in basalt-fiber-reinforced composites: tailoring the fiber-matrix interface, Compos. Part B Eng. 192 (2020) 108011.
[41] X. Sun, Z. Gao, P. Cao, C. Zhou, Mechanical properties tests and multiscale numerical simulations for basalt fiber reinforced concrete, Constr. Build. Mater. 202 (2019) 58–72.
[42] D.R. Askeland, P.P. Fulay, W.J. Wrigh, The Science and Engineering of Materials, sixth ed., Cengage Learning, Stamford, CT, 2011.